

ASTROMETRIC RADIAL VELOCITIES FROM HIPPARCOS

Dainis Dravins¹, Lennart Lindegren¹, Søren Madsen², Johan Holmberg¹

¹Lund Observatory, Box 43, SE-22100 Lund, Sweden

²Copenhagen University Observatory, Juliane Maries Vej 30, DK-2100 Copenhagen, Denmark

ABSTRACT

Space astrometry now permits accurate determinations of stellar radial motion, without using spectroscopy. Using Hipparcos data, this is possible for stars in nearby moving clusters, where all stars share nearly the same space velocity. A maximum-likelihood method has been developed to yield kinematic cluster parameters (including the internal velocity dispersion) purely from parallaxes and proper motions. The deduced astrometric radial velocities of the Ursa Major open cluster and the Hyades have inaccuracies of 0.3 and 0.4 km s⁻¹, respectively, and the internal cluster velocity dispersions are found to be 0.66 ± 0.10 and 0.25 ± 0.04 km s⁻¹ (consistent with random stellar motions). Remaining errors arise from uncertainties in excluding binary stars. The errors get worse for the more distant Coma Berenices cluster.

The fitting of cluster parameters includes all individual stellar distances. The constraint of a uniform average cluster velocity markedly improves the parallax precisions (roughly by a factor two), compared with Hipparcos data for individual stars. The HR diagram for the Hyades now reveals a very narrow main sequence line (not band), even suggesting some wiggles in it.

Discrepancies between astrometric and spectroscopic radial velocities reveal effects (other than stellar motion) that affect wavelength positions of spectral lines. Such are caused by stellar pulsation, surface convection, and by gravitational redshifts. A parallel programme is obtaining and analysing high-precision spectroscopic radial velocities for different classes of spectral lines in these programme stars.

Key words: radial velocities; Hipparcos; Hyades; open clusters.

1. SPECTROSCOPIC VERSUS ASTROMETRIC RADIAL VELOCITIES

Wavelengths of stellar spectral lines (originating in stellar surface layers) depend not only on the star's velocity. Intrinsic line asymmetries and shifts are

caused by, for example, atmospheric pulsation, surface convection, deviant isotopic composition, pressure shift, and gravitational redshift. In ordinary stars, the discrepancy between the apparent velocity inferred from the spectrum (by applying the Doppler principle), and the true centre-of-mass motion, is expected to be no more than about one km s⁻¹, but increasing to tens of km s⁻¹ in white dwarfs (due to gravitational redshifts) and in supergiants (due to expanding atmospheres). Thus, unless corrected for, merely varying atmospheric lineshifts between different stars will mimic a kinematic velocity dispersion.

Previously, the discrepancy between spectroscopic radial velocities and the astrometrically determined stellar motion has been known only for the Sun. Solar motion is known from planetary system dynamics and does not depend on spectroscopic data. Thus, it has been possible to interpret solar lineshifts as originating from gravitational redshift, convective blueshifts, and other atmospheric phenomena (Dravins et al. 1981, 1986; Nadeau 1988). For other stars, only studies of the *relative* lineshifts between stars sharing the same average motion have been possible, for example deducing gravitational redshifts in white dwarfs that are members of binary systems or between cluster stars sharing the same system velocity (e.g. Reid 1996)

Convective lineshifts originate from correlated velocity and brightness patterns: rising (blueshifted) elements are hot (bright), and normally a net blueshift results from a larger contribution of such blueshifted photons than of redshifted ones from the sinking and cooler (darker) gas. For the Sun, the effect is typically 0.3 km s⁻¹, but varies among different classes of spectral lines. The blueshifts increase for weaker lines (formed deeper into the convective layers); for ionized lines, and such of high excitation potential (formed mostly in the hotter and rising elements); and at shorter wavelengths (where the black-body contrast for a certain temperature difference increases). In the vacuum ultraviolet, the sign reverses to redshifts of ≈ 1 km s⁻¹ (lines are now formed in the region of convective overshoot, with an inverted velocity/brightness correlation; Samain 1991).

Stars of different temperature and luminosity are predicted to have different amounts of convective lineshift. Convective blueshift increases with temperature, and also with luminosity. The vigorous granulation in F-stars is expected to cause blueshifts of

$\approx 1 \text{ km s}^{-1}$, while those in a cooler K dwarf may amount to only $\approx 0.2 \text{ km s}^{-1}$ (Dravins & Nordlund 1990; Dravins 1992). The values for giants are unknown, but could be rather higher, as also indicated by studies of the relative shifts between different types of lines in the same star (Nadeau & Maillard 1988).

Such lineshifts are not necessarily constant in time. Magnetic fields disturb surface convection, and granules may not develop to equally large size or velocity amplitude, causing cyclic changes in line wavelengths with the stellar activity cycle. This has implications in searches for exoplanets with comparable periods. Since the presence of a planet is inferred from slight cyclic changes in stellar wavelengths (interpreted as caused by stellar motion), any credible identification of exoplanets with orbital periods comparable to such an activity-cycle period requires a careful segregation of non-velocity effects.

Empirically determined ‘spectral-class-dependent corrections’, and similar, are often applied to force spectroscopic velocity measurements of, e.g., earlier- and later-type stars into agreement. Even after such an ‘adjustment’, the zero point for velocity remains indeterminate. That is often obtained by calibrating against sunlight, setting its velocity to ‘0’ (with or without corrections for the solar gravitational redshift of 0.636 km s^{-1}). The remaining *inaccuracy* inherent in all spectroscopic radial velocities must be on the order of 0.5 km s^{-1} even if the measuring *imprecision* is orders of magnitude smaller. In contrast, astrometric radial velocities (at least in principle) permit a calibration of stellar radial velocity measurements in absolute units, irrespective of spectral complexity.

The aim of the present project is to perform an astrometric determination of the radial velocities of stars in nearby open clusters, and thus to obtain the true radial motions for stars of different spectral types and rotational velocities. For these programme stars, a programme is in progress to precisely measure also their spectroscopic velocities, using the ELODIE radial-velocity instrument at Haute-Provence Observatory. Different correlation templates are applied for different classes of spectral lines (Gullberg & Dravins 1998), with the aim to identify non-velocity shifts in different stars; to study stellar surface granulation (through convective lineshifts), of stellar interiors (through gravitational redshifts), and to generally improve the absolute accuracy in radial-velocity measurements (especially for early-type stars with rapid rotation or otherwise complex spectra).

2. ASTROMETRIC SIGNATURES OF RADIAL VELOCITY

For any star, its component of radial motion may become visible as a secular change in its parallax and proper motion. The theoretical possibility of astrometrically deducing radial velocities from such geometric projection effects was realized already a very long time ago, perhaps first by Bessel in the 19th century, discussed by Schlesinger (1917) and others, before actually applied in a few special cases of stars

where secular changes in their very large proper motion could be measured (Gatewood & Russell 1974). However, only with Hipparcos has the accuracy of the method reached a level ($< 1 \text{ km/s}$) permitting a meaningful search for differences to spectroscopic velocities.

Moving clusters, in which the stars are assumed to have a common motion relative to the Sun, offer a special possibility to determine radial velocities purely from astrometric data. The principle can be understood as follows (Figure 1): as the cluster moves in the radial direction, it appears to contract or expand due to perspective. This relative rate of contraction equals the relative rate of change in distance to the cluster. This can be converted to a linear velocity (in km s^{-1}) if the distances to the cluster stars are known, e.g. from trigonometric parallax.

In essence, this inverts the classical problem of determining the cluster distance from proper motions and radial velocities, which (due to geometric projection effects) change across the angle subtended by the cluster. With the distance accurately known, one solves the problem for the radial velocity instead.

We will now formulate this principle mathematically and show how the maximum-likelihood method can be applied to determine the kinematic parameters of a moving cluster, in particular the space velocity of the cluster centroid and the internal velocity dispersion. From the space velocity of the cluster, the radial velocities of the individual member stars can then be calculated (apart from the radial component of the internal dispersion) independent of spectroscopic data. Using parallaxes and proper motions obtained with the Hipparcos satellite, such astrometric radial velocities are here for the first time obtained for numerous stars in the Hyades, the Ursa Major cluster, and Coma Berenices.

3. ESTIMATION OF CLUSTER PARAMETERS

3.1. Astrometric Observations

For each observed star in a cluster, $i = 1 \dots n$, the Hipparcos Catalogue (ESA 1997) provides five astrometric parameters: two for the position at the catalogue epoch 1991.25 (α_i , δ_i), the trigonometric parallax (ϖ_i), and two components of the proper motion (μ_{α^*i} , $\mu_{\delta i}$). The catalogue also provides the standard deviations and correlations of all these data. For our purpose the positional data are regarded as error-free and defining the barycentric direction \mathbf{r}_i towards the star. Two more auxiliary unit vectors are computed from the positional data: \mathbf{p}_i in the local direction of increasing right ascension (‘East’), and \mathbf{q}_i in the local direction of increasing declination (‘North’); these define the directions of the equatorial components of the proper motion. An expression for the orthogonal triad \mathbf{p}_i , \mathbf{q}_i , \mathbf{r}_i is given by Equation 1.5.72 in Volume 1 of the Hipparcos Catalogue (ESA 1997).

The proper motions and parallaxes, in contrast to the positions, have observational errors which must be taken into account by the estimation algorithm. For a given star we define a column matrix of ob-

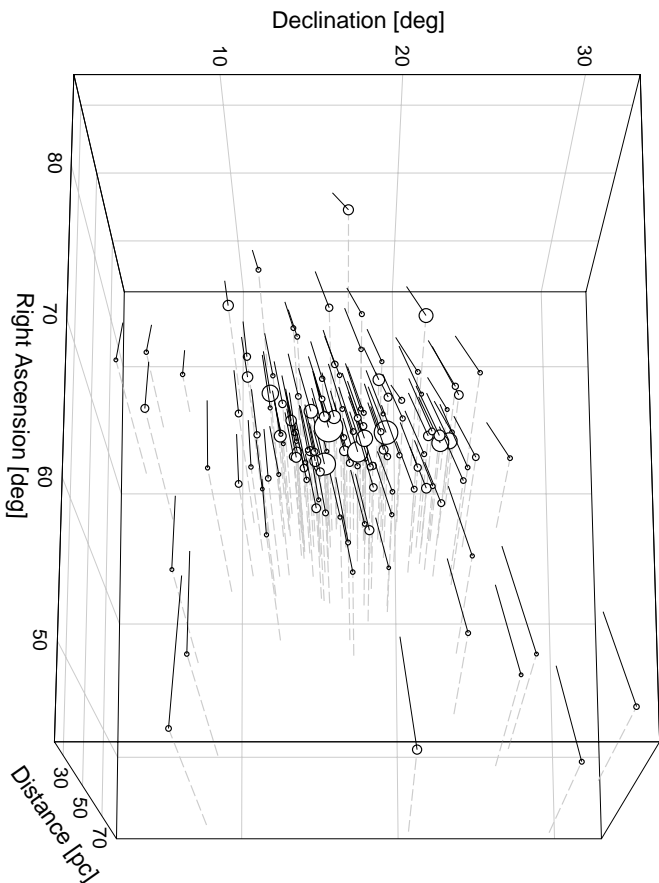


Figure 1. The principle of determining astrometric radial velocities. Stars in a moving cluster share the same mean velocity vector. Parallaxes give the distance, while proper-motion vectors show the fractional change with time of the cluster’s angular size. The latter equals the time derivative of distance, or the radial velocity. This plot shows positions for single stars in the Hyades, together with their measured distances and proper motions (shown over 100 000 year-s).

servables, $\mathbf{a}_i = [\varpi_i \mu_{\alpha^*i} \mu_{\delta i}]^T$ (where the prime denotes matrix transposition), and express their uncertainties and correlations by means of the 3×3 covariance matrix $\mathbf{C}_i = E[(\tilde{\mathbf{a}}_i - \bar{\mathbf{a}}_i)(\tilde{\mathbf{a}}_i - \bar{\mathbf{a}}_i)^T]$. Here, $\tilde{\mathbf{a}}$ stands for the observed value of the generic variable \mathbf{a} , as opposed to the true value ($\bar{\mathbf{a}}$) and estimated ($\hat{\mathbf{a}}$) values. Units are milliarsec (mas) for the parallax, mas yr $^{-1}$ for the proper motion components (with 1 yr = 365.25 days), and km s $^{-1}$ for linear velocities. In this system the astronomical unit is $A = 4.74047$ km yr s $^{-1}$.

3.2. Modelling the Data

The application of statistical estimation methods such as maximum likelihood or Bayesian techniques requires that the observables (\mathbf{a}_i , $i = 1 \dots n$) are modelled as random variables with a probability density function (pdf) depending on a finite set of model parameters. The model must include both the physical object (e.g. random motions in the cluster) and the process of observation (i.e. observational errors).

In the present model we assume that the individual space velocities, \mathbf{v}_i , follow a trivariate gaussian distribution with mean value \mathbf{v}_0 (the ‘centroid velocity’) and standard deviation σ_v in each coordinate (the internal velocity dispersion). Thus \mathbf{v}_0 and σ_v are model parameters to be fitted to the observations. Additionally, the distances to the individual stars are regarded as model parameters, or (equivalently) the parallaxes ϖ_i . The total number of model parameters is $n + 4$.

The pdf for $\tilde{\mathbf{a}}_i$ is denoted $f(\tilde{\mathbf{a}}_i)$. Details of its derivation will be published elsewhere (Dravins et al. 1998). In summary, we find:

$$f(\tilde{\mathbf{a}}_i) = (2\pi)^{-3/2} |\mathbf{D}_i|^{-1/2} \times \exp \left[-\frac{1}{2} (\tilde{\mathbf{a}}_i - \mathbf{c}_i)^T \mathbf{D}_i^{-1} (\tilde{\mathbf{a}}_i - \mathbf{c}_i) \right] \quad (1)$$

where:

$$\mathbf{c}_i = \begin{bmatrix} \varpi_i \\ p_i^0 \varpi_i / A \\ q_i^0 \varpi_i / A \end{bmatrix} \quad (2)$$

$$\mathbf{D}_i = \mathbf{C}_i + \begin{bmatrix} 0 & 0 & 0 \\ 0 & (\sigma_v \varpi_i / A)^2 & 0 \\ 0 & 0 & (\sigma_v \varpi_i / A)^2 \end{bmatrix} \quad (3)$$

Note that the *observed* parallax and proper motion enter only through the vector $\tilde{\mathbf{a}}_i = [\tilde{\varpi}_i \tilde{\mu}_{\alpha^*i} \tilde{\mu}_{\delta i}]$, while \mathbf{c}_i and \mathbf{D}_i depend on the *model parameter* ϖ_i .

3.3. Maximum-Likelihood Estimation

Writing the pdf f in Equation 1 as conditional upon the model parameters, the log-likelihood function is:

$$L(\boldsymbol{\varpi}, \mathbf{v}_0, \sigma_v) = \ln \prod_{i=1}^n f(\tilde{\mathbf{a}}_i | \varpi_i, \mathbf{v}_0, \sigma_v) \quad (4)$$

where $\boldsymbol{\varpi}$ is the column matrix of the n model parameters ϖ_i . The maximum likelihood (ML) estimate $(\hat{\boldsymbol{\varpi}}, \hat{\mathbf{v}}_0, \hat{\sigma}_v)$ is obtained by finding the maximum of L . Since the covariances \mathbf{C}_i are independent of the model parameters, this is equivalent to minimising:

$$G(\boldsymbol{\varpi}, \mathbf{v}_0, \sigma_v) = \sum_{i=1}^n \ln |\mathbf{C}_i^{-1} \mathbf{D}_i| + \sum_{i=1}^n g_i \quad (5)$$

where the first term depends only on σ_v , and:

$$g_i(\boldsymbol{\varpi}_i, \mathbf{v}_0, \sigma_v) = (\tilde{\mathbf{a}}_i - \mathbf{c}_i)' \mathbf{D}_i^{-1} (\tilde{\mathbf{a}}_i - \mathbf{c}_i) \quad (6)$$

is a non-negative measure of discrepancy for each star. From Monte Carlo simulations of the ideal conditions (assuming no contaminating field stars or binaries) we find that g_i is approximately distributed as χ_2^2 . Thus, $g_i > 9$ may be a reasonable criterion for detecting outliers, the significance level being $\simeq 0.01$. Standard minimisation algorithms (Press et al. 1992) have been used to solve the minimisation problem.

Monte Carlo simulations are essential for studying the precision of the ML estimate and its possible biases. From extensive simulations we conclude that the estimates of $\boldsymbol{\varpi}$ and \mathbf{v}_0 are almost unbiased, while σ_v is severely underestimated by the ML estimator. We remedy this by creating synthetic data sets, with all parameters set equal to the ML estimates from the real data, except that the synthetic σ_v is gradually increased until its ML estimate agrees with that from the real data. This synthetic σ_v is then regarded as an unbiased estimate of the velocity dispersion. Such simulations also provide bias corrections to \mathbf{v}_0 , typically about 0.1 km s^{-1} . The bias corrections and precision estimates given below were based on sets of 1000 experiments.

Our formulation of the ML problem does not take into account field stars not sharing the common motion of the cluster stars, although such an extension would in principle be possible. Consequently the method should only be applied to the actual members of the cluster, or, more precisely, to members whose mean space velocities during the Hipparcos mission can be modelled according to our assumptions. In practice this rules out a number of close binaries, even if they are members of the cluster, since the short-term motion of the photocentre of such an object may deviate significantly from the motion of its centre of mass. Such objects will normally show up as outliers in the minimisation process.

4. RADIAL-VELOCITY RESULTS

4.1. The Hyades

A detailed study of the distance, structure, dynamics and age of the Hyades, for the first time using the Hipparcos data, has been made by Perryman et al. (1997). Of particular interest here is the heliocentric position and velocity of the cluster centroid derived in that paper from a combination of astrometric and available spectroscopic (radial velocity) data. For the inner 20 pc, using 180 stars, they find the centroid position $\mathbf{b}_0 = (+17.72, +41.16, +13.32) \text{ pc}$ and centroid velocity $\mathbf{v}_0 = (-6.32, +45.24, +5.30) \text{ km s}^{-1}$ when expressed in the equatorial (ICRS) system. Furthermore, they estimate the true internal velocity dispersion, near the centre, to be in the range 0.2 to 0.3 km s^{-1} .

Table 1. Estimates of the space velocity of the Hyades using different stellar samples of size n . $(\hat{v}_{0x}, \hat{v}_{0y}, \hat{v}_{0z})$ are the equatorial components of $\hat{\mathbf{v}}_0$ in km s^{-1} . $\hat{\sigma}_v$ is the internal velocity dispersion in km s^{-1} . These data are not corrected for statistical biases (cf. Table 2).

Sample	n	\hat{v}_{0x}	\hat{v}_{0y}	\hat{v}_{0z}	$\hat{\sigma}_v$
all	195	-5.99	+45.66	+5.44	0.98
A	133	-6.08	+45.91	+5.56	0.15
B	132	-5.65	+46.18	+5.59	0.94
C	133	-6.16	+45.01	+5.25	0.73
AB	98	-6.10	+45.78	+5.51	0.15
AC	100	-5.98	+45.95	+5.58	0.14
BC	104	-5.88	+45.66	+5.42	0.51
ABC	88	-5.97	+45.87	+5.55	0.14

The preliminary results of our analysis, using exclusively Hipparcos measurements, are shown in Table 1. Since the selection of kinematically representative member stars is critical, we made solutions for several different stellar samples, using criteria described below. A more definitive selection will be possible after additional examination of spectroscopic data in conjunction with an ongoing observational programme (Gullberg & Dravins 1998).

The list of stars originally proposed for this study was compiled in 1982 from a variety of sources in order to ensure that as many members as possible would be included. From the Hipparcos data, and also from radial velocity data published since, it is however obvious that several of the stars on that list cannot reasonably be members of the Hyades cluster. Since all the stars were already considered and discussed by Perryman et al. (1997) we retain, as a first approximation, only the stars positively classified as members ($S = 1$) in their (provisional) Table 2. This gave a sample of 195 stars as basis for our further selection.

The results from applying the ML algorithm to all the presumed member stars, i.e. without rejection of outliers, are shown in the first row of Table 1. The method provides estimated parallaxes which should be more precise than the observed values. Figure 2a shows the HR diagram for the 195 stars with absolute magnitudes computed from the observed parallaxes, i.e. using $M_{Hp} = Hp + 5 \log(\tilde{\varpi}_i/100)$. This is nearly equivalent to a corresponding HR diagram in Perryman et al. (1997). For comparison, Figure 2b shows the HR diagram for the same 195 stars but with M_{Hp} calculated from the *estimated* parallaxes $\hat{\varpi}_i$. The main sequence in Figure 2b is clearly much better defined, especially towards the faint end, where the uncertainties in the observed parallaxes become significant. This is a good indication that there is a sound physical basis for the model.

It is noted that the estimated velocity dispersion is quite large, possibly indicating strong contamination by outliers. This is confirmed by the distribution of g_i values, where 11 per cent are > 9 . A cleaner sample ('A' in Table 1) was therefore obtained by successively removing the stars with the largest g_i ,

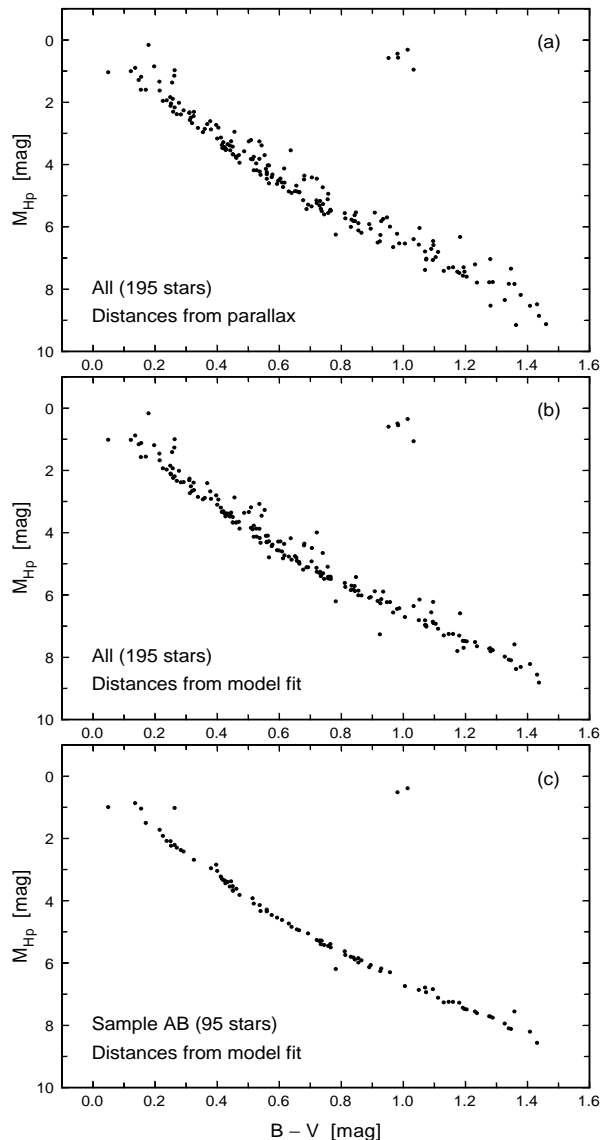


Figure 2. The HR diagram for the Hyades, using data for all the presumed member stars in our sample (a and b), and for the subset of 98 stars with a good model fit, where known spectroscopic binaries were also excluded (c). In (a) the observed parallaxes were used to compute absolute magnitudes, in (b) and (c) the estimated parallaxes from the model fitting.

and recalculating the solution, until all $g_i \leq 9$. This caused only a small adjustment of \hat{v}_0 , while the estimated velocity dispersion became very small.

Many of the stars in the Hyades are known to be spectroscopic binaries, and many of these could very well have deviating proper motions as measured by Hipparcos. An alternative sample ‘B’ was therefore derived by eliminating all stars identified as spectroscopic binaries in Perryman et al. (1997). This gave nearly the same number of stars as in sample A, but the selection is in fact quite different: the intersection of ‘A’ and ‘B’, referred to as sample ‘AB’ in Table 1, contains only 60 per cent of the union of stars in ‘A’ and ‘B’. The results for ‘B’ and ‘AB’ are also given

Table 2. Adopted estimates and uncertainties of the space velocities and velocity dispersions for the three clusters. The estimates in this table have all been corrected for statistical biases through Monte Carlo simulations. All values are in km s^{-1} .

Cluster	n	v_{0x}	v_{0y}	v_{0z}	σ_v
Hyades (A)	133	-6.07 ± 0.13	$+45.77$ ± 0.36	$+5.53$ ± 0.11	0.25 ± 0.04
Ursa Major	23	$+7.86$ ± 0.21	-12.00 ± 0.17	-8.48 ± 0.27	0.66 ± 0.10
Coma Ber.	25	-3.47 ± 2.03	$+4.54$ ± 0.23	-2.71 ± 0.99	< 0.24

in Table 1.

The HR diagram for sample ‘AB’ with absolute magnitudes calculated from the estimated parallaxes is shown in Figure 2c. The main sequence is remarkably well-defined in this diagram, indicating that most binaries, at least with a not too large Δm , have been removed. The small scatter among the main-sequence stars indicates that the estimated parallaxes $\hat{\varpi}_i$ in this sample are about a factor two more precise than the observed values.

The third selection, sample ‘C’, was made by means of the HR diagram in Figure 2b. A curve was drawn by eye and hand through what appears to be the main sequence, and only stars with absolute magnitude within ± 0.2 mag of the curve were retained, plus the four stars on the well-defined giant branch. Although this sample contains nearly the same number of stars as ‘A’ or ‘B’, its overlap with each of these samples is only about 75 per cent. The kinematic results for ‘C’ and its intersections with the other samples are given in Table 1.

A closer analysis of the various samples leads to the conclusion that sample ‘A’ probably gives the most reliable solution, as it contains the maximum number of stars which are consistent with the model. Biases and uncertainties of this solution were estimated with the Monte Carlo technique described in Section 3.3. The corrected results, with standard errors, are given in Table 2. The corresponding radial velocity of the cluster centroid is $v_{0r} = \mathbf{r}'_0 \mathbf{v}_0 = +39.57 \pm 0.42 \text{ km s}^{-1}$ (where $\mathbf{r}_0 = \mathbf{b}_0/b$ is its heliocentric direction).

4.2. The Ursa Major Cluster

From our original proposal, 17 stars in the Ursa Major cluster were observed by Hipparcos. A direct search of the Hipparcos Catalogue for stars with parallaxes and proper motions in general agreement with the space motion of these 17 stars, within a radius of 25 pc, yielded eight more candidates. One of them was later rejected on the basis of its radial velocity, and another as having $g_i > 9$. The result from a solution with the remaining 23 stars, including bias corrections, is in Table 2. This solution is very pre-

liminary, as the memberships of a few stars remain to be confirmed by spectroscopic radial velocities. The uncertainties in the components of \mathbf{v}_0 translate to an uncertainty of about 0.3 km s^{-1} in the radial direction.

4.3. The Coma Berenices Cluster

This cluster is the most distant of the three ($b_0 \simeq 87 \text{ pc}$). Its small angular radius ($\simeq 3^\circ$) and low velocity relative to the Sun ($\simeq 6 \text{ km s}^{-1}$) combine to make it less suitable for the present method. Of the originally proposed 40 stars, five were rejected because of discrepant parallaxes, assuming that the linear size of the cluster is approximately the same in all directions, and one was rejected because of its location quite far from the centre, as projected on the sky. Applying the ML algorithm to the remaining 34 stars, nine more were successively rejected as having $g_i > 9$. The solution for the 25 accepted stars is shown in Table 2. For the internal velocity dispersion only an upper limit of 0.24 km s^{-1} (one σ) could be derived. Putting the cluster centroid at $(-79.0, -7.9, +38.5) \text{ pc}$, its radial velocity becomes $+1.5 \pm 2.3 \text{ km s}^{-1}$.

5. SYSTEMATIC INTERNAL MOTIONS

A required assumption (just as in the classical problem of distance determination from measured radial velocities) is that all cluster stars share the same velocity vector, apart from the random internal motions. Elementary dynamical considerations indicate that the random motions, and those due to expansion, rotation, etc., should be only a fraction of one km s^{-1} , unless the clusters are dispersing. The random component of the internal velocity dispersion is included in the model described previously. However, systematic velocity patterns are not included and it is conceivable that such could bias the determination of the astrometric radial velocities.

For the derivation of Equation 1 we assumed $E(\mathbf{v}_i) = \mathbf{v}_0$. In a first-order analysis of the effects of systematic velocities we may replace this assumption with a velocity field in which the mean velocity depends on position \mathbf{b} according to:

$$E(\mathbf{v}_i) \equiv \mathbf{u}(\mathbf{b}_i) = \mathbf{v}_0 + \mathbf{T}(\mathbf{b}_i - \mathbf{b}_0) \quad (7)$$

where $\mathbf{T} = \partial \mathbf{u} / \partial \mathbf{b}'$. With respect to a given reference frame the tensor \mathbf{T} is described by the nine gradients $T_{jk} = \partial u_j / \partial b_k$, $j, k = x, y, z$. \mathbf{T} in general includes rigid-body rotation as well as expansion/contraction and linear shear along an arbitrary plane. A detailed analysis of this problem (Dravins et al. 1998) shows that all components of \mathbf{T} are in principle observable, with the exception of the single component representing a uniform and isotropic dilation of the cluster. If the cluster expands at a rate K , then the corresponding bias in the centroid radial velocity will be $\Delta v = -\mathbf{b}_0 K$. All other systematic velocity patterns would be revealed by systematic patterns of the proper motion residuals, and could in principle be included as additional model parameters.

A reasonable upper limit on the expansion rate is the inverse age of the cluster. For the Hyades, an age of 625 Myr (Perryman et al. 1997) corresponds to an upper limit of $K = 0.0015 \text{ km s}^{-1} \text{ pc}^{-1}$, corresponding to a bias of -0.07 km s^{-1} in the astrometric radial velocity for the cluster centroid.

The sensitivity of the Hyades solution to cluster rotation and shear was studied by Monte Carlo simulations. An upper limit to the cluster rotation is given by the circular velocity at, say, 10 pc from the centroid, while an upper limit to the shear may be set by the galactic differential rotation, locally given by Oort's constant A . Both assumptions give upper limits to the radial velocity bias of the order of 0.5 km s^{-1} . Actually the velocity fields corresponding to these upper limits would produce strong and characteristic signatures in the residuals. There is no evidence for any such effect in the data, nor in the three-dimensional velocity residuals considered by Perryman et al. (1997). Thus we conclude that the probable effects on the estimated radial velocities are several times smaller than these limits and therefore insignificant compared with the statistical uncertainties.

ACKNOWLEDGMENTS

We wish to thank M.A.C. Perryman for discussions concerning the kinematics of the Hyades and for providing membership data for this cluster in advance of publication. This project is supported by the Swedish National Space Board and the Swedish Natural Science Research Council.

REFERENCES

- Dravins, D., 1992, in M.H. Ulrich, ed.: High Resolution Spectroscopy with the Very Large Telescope, European Southern Observatory, p. 55
- Dravins, D., Larsson, B., Nordlund, Å., 1986, A&A 158, 83
- Dravins, D., Lindegren, L., Madsen, S., Holmberg, J., 1998, A&A, in preparation
- Dravins, D., Lindegren, L., Nordlund, Å., 1981, A&A 96, 345
- Dravins, D., Nordlund, Å., 1990, A&A 228, 203
- ESA, 1997, The Hipparcos and Tycho Catalogues, ESA SP-1200
- Gatewood, G., Russell, J., 1974, AJ 79, 815
- Gullberg, D., Dravins, D., 1998, in preparation
- Nadeau, D., 1988, ApJ 325, 480
- Nadeau, D., Maillard, J.P., 1988, ApJ 327, 321
- Perryman, M.A.C., Brown, A.G.A., Lebreton, Y., et al., 1997, A&A, in press
- Press, W.H., Teukolsky, S.A., Vetterling, W.T., Flannery, B.P., 1992, Numerical Recipes in Fortran (2nd ed.), Cambridge Univ. Press
- Reid, I.N., 1996, AJ 111, 2000
- Samain, D., 1991, A&A 244, 217
- Schlesinger, F., 1917, AJ 30, 137